Reconfiguring active particles by electrostatic imbalance

Jing Yan[1†], Ming Han[2†], Jie Zhang[1], Cong Xu[1], Erik Luijten[3]★ and Steve Granick[4]★

Active materials represent a new class of condensed matter in which motile elements may collectively form dynamic, global structures out of equilibrium[1-3]. Here, we present a general strategy to reconfigure active particles into various collective states by introducing imbalanced interactions. We demonstrate the concept with computer simulations of self-propelled colloidal spheres, and experimentally validate it in a two-dimensional (2D) system of metal–dielectric Janus colloids subjected to perpendicular a.c. electric fields. The mismatched, frequency-dependent dielectric responses of the two hemispheres of the colloids allow simultaneous control of particle motility and colloidal interactions. We realized swarms, chains, clusters and isotropic gases from the same precursor particle by changing the electric-field frequency. Large-scale polar waves, vortices and jammed domains are also observed, with the persistent time-dependent evolution of their collective structure evoking that of classical materials. This strategy of asymmetry-driven active self-organization should generalize rationally to other active 2D and three-dimensional (3D) materials.

The evolution of modern colloid study presents examples of ever-increasing complexity of using them as models for other systems. Originally, homogeneous spheres gave insight into atomic organization into crystals, glasses and their structural defects[4]. The paradigm shifted to patchy colloids whose anisotropic interactions allow them to self-assemble into complex 'molecular colloids'[5]. Most recently, self-propelled colloids have started to mimic nonequilibrium dynamics in nature such as flocks of birds and colonies of bacteria[2,6–8]. Many forms of collective self-organization have been identified with active particles[2,7] and molecules[3,9]. An important open question remains: Might one synthetically program multiple desired modes of collective behaviour into the same active particle? Such programmability could represent a rudimentary form of multi-tasking potentially useful for applications[10,11], and by presenting the capability of differentiation, although reversibly so and with the capacity for reconfiguration, would extend the metaphor[1–3,7] that active systems can be designed to emulate living systems.

To realize such reconfigurable active particles, we employ swimming Janus colloids, which are particles with two distinct hemispheres[12–14] that present a prototypical synthetic material with the capacity to self-propel[6,15,16] thanks to inherent broken symmetry. The Janus feature also allows independent control of the material properties of the two hemispheres, providing a rich design space for colloid–colloid interactions. Figure 1a summarizes our strategy. For simplicity and generality in illustrating

this concept, consider self-propelled particles with two electric charges, one each on the head and tail. To be more concrete in this presentation, we begin with 3D molecular dynamics (MD) simulations of such particles, without loss of generality in the overdamped regime (Fig. 1b–d and Supplementary Movies 1–3). When the two charges have the same sign and comparable magnitude, the particles act similarly to isotropic spheres and have random configurations. This gas state similarly emerges when the electrostatics are negligible. As imbalance between two charges kicks in, various forms of non-trivial self-organization arise. As a first possibility, swimmers with equal-and-opposite charges on each hemisphere can polymerize into connected chains (Fig. 1b). The equilibrium thermodynamics of dipolar chains has been extensively studied[17]; this would be the motile analogue: active chains. Second, if the charge on one hemisphere greatly exceeds that on the other, a torque arises when active spheres come into proximity. This torque diverts head-repulsive swimmers to avoid head-to-head collisions, and temporarily aligns two colliding swimmers in the same direction. The resulting two-particle alignment can produce coherent swarming of many particles on a large scale (Fig. 1c). The phenomenology is qualitatively described by the classic Vicsek model[18], except that here velocity correlations result from this new reorientation mechanism. On the other hand, tail-repulsive particles in proximity will preferentially position their tails apart, thus encouraging them to face each other to form jammed clusters of high local density (Fig. 1d). This is generally consistent with the density-dependent mobility model[19]. However, different from other clustering systems based on velocity reduction during collisions[20] or interparticle attraction[7], reorientation dynamics in this system determines and accelerates the cluster formation process.

How to implement these ideas experimentally? We turn to dipolar interactions that can be easily induced and tuned by external electric fields[21]. Specifically, we select Janus particles prepared from silica spheres with one hemisphere coated with metal, covered with a thin SiO_2 protective layer so that the outermost chemical makeup of the particles is homogeneous. Particles with relatively large size (3 μm) allow visualization of the double-faced feature by optical microscopy, as well as minimize thermal motion. In deionized water, they settle to the bottom of the planar sample cell while remaining laterally mobile (Fig. 2a). The application of a.c. electric fields perpendicular to this quasi-2D system causes the particle equators to orient vertically while polarizing the hemispheres. Importantly, the metal and silica hemispheres polarize differently. This imbalance has two consequences. First, ionic flows, excited by the local electric field near the particle surface, have different magnitudes on the two sides and lead to self-propulsion of these

[1]Department of Materials Science and Engineering, University of Illinois, Urbana, Illinois 61801, USA. [2]Applied Physics Graduate Program, Northwestern University, Evanston, Illinois 60208, USA. [3]Departments of Materials Science and Engineering, Engineering Sciences and Applied Mathematics, and Physics and Astronomy, Northwestern University, Evanston, Illinois 60208, USA. [4]IBS Center for Soft and Living Matter, UNIST, Ulsan 689-798, South Korea. [†]These authors contributed equally to this work. *e-mail: luijten@northwestern.edu; sgranick@ibs.re.kr
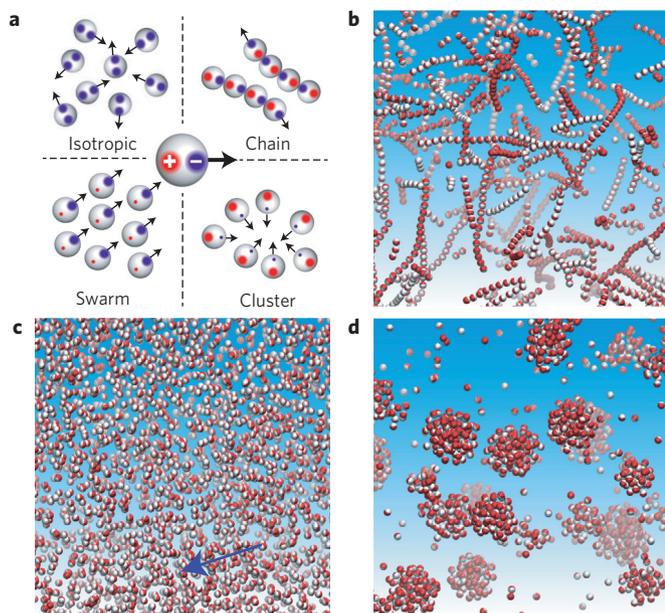
Figure 1 | Examples of collective active states formed by spheres with imbalanced, off-centred charges. a, The strategy is to program dual electric charges shifted from the sphere centre onto opposing hemispheres. Their signs (positive and negative) are colour coded (red and blue), their relative magnitude is indicated by the respective dot size, and black arrows indicate the swimming direction of the spheres. **b–d**, Representative 3D simulated structures of active chains (**b**), swarms (**c**) and clusters (**d**). White hemispheres represent the leading sides and red hemispheres the trailing sides. The blue arrow in **c** marks the global direction of the swarm.

Figure 2 | Experimental realization of the predicted active states from the same Janus colloidal spheres. a, Experimental set-up: Janus spheres are allowed to sediment in water between two electrodes. An a.c. electric field *E* is applied in the *z*-direction to cause particles to swim in the *x*–*y* plane. **b**, Calculated real and imaginary dipole coefficients *K* (solid and dashed lines, respectively) plotted against frequency *f* for dielectric (blue) and metallic (red) hemispheres. Frequencies indicated by vertical lines are used in the experiments (5 kHz, 30 kHz and 1 MHz, respectively). **c**, Calculated dipolar interaction U'_{AB} at contact for different interaction pairs shown on the right, normalized by the interaction between two purely metallic hemispheres at infinite frequency. **d–g**, Illustrative images of gas (**d**), swarms (**e**), chains (**f**) and clusters (**g**) observed experimentally. Images **d–f** are obtained in deionized water at the frequencies marked in **b** and **c**. The cluster phase (**g**) is obtained in 0.1 mM NaCl solution at $f = 40$ kHz. Scale bars are 5 μm in **d–f** and 30 μm in **g**.

particles perpendicular to the field, a phenomenon known as induced-charge electrophoresis (ICEP)[15]. Second, the differential dielectric responses lead to different dipole moments for the leading and trailing hemispheres, providing the opportunity to achieve the imbalanced electrostatics that we have envisioned. Given that these dipoles are all located in and oriented perpendicular to the sample plane, the resulting dipole–dipole interactions are isotropic in the plane and act analogously to charge–charge interactions, so our previous predictions should apply in this experimental system. More importantly, the frequency-dependent dielectric response makes it possible to simultaneously control not only the imbalance between the dipole moments of the two hemispheres, but also the swimming force, and even the direction of self-propulsion, by a single parameter, the electric-field frequency *f*. We calculate the dielectric spectra for both hemispheres as well as the interactions between the hemispheres in Fig. 2b,c, taking into account both the intrinsic material properties and the response of ions in the electric double layer[22] (see Supplementary Discussion 1). The dependence of particle velocity on frequency is also measured (Supplementary Fig. 1 and Supplementary Discussion 2), showing that particles undergo a reversal in swimming direction as the frequency is increased.

By varying the electric-field frequency, we realize all the regimes predicted by the heuristic arguments of Fig. 1a. First, when *f* is low (∼kHz), dipolar interactions are negligible due to strong ionic screening effects, hence the particles move and collide randomly and isotropically[16] (Fig. 2d and Supplementary Movie 4). As *f* increases moderately to 20–50 kHz (Supplementary Movies 5 and 6), ionic screening is largely reduced, such that colloids can interact with each other through dipolar interactions. At the same time, the particles reverse their swimming directions, with their metallic side facing forwards. Therefore, the condition for swarming is fulfilled: the repulsion between the leading, metallic hemispheres dominates
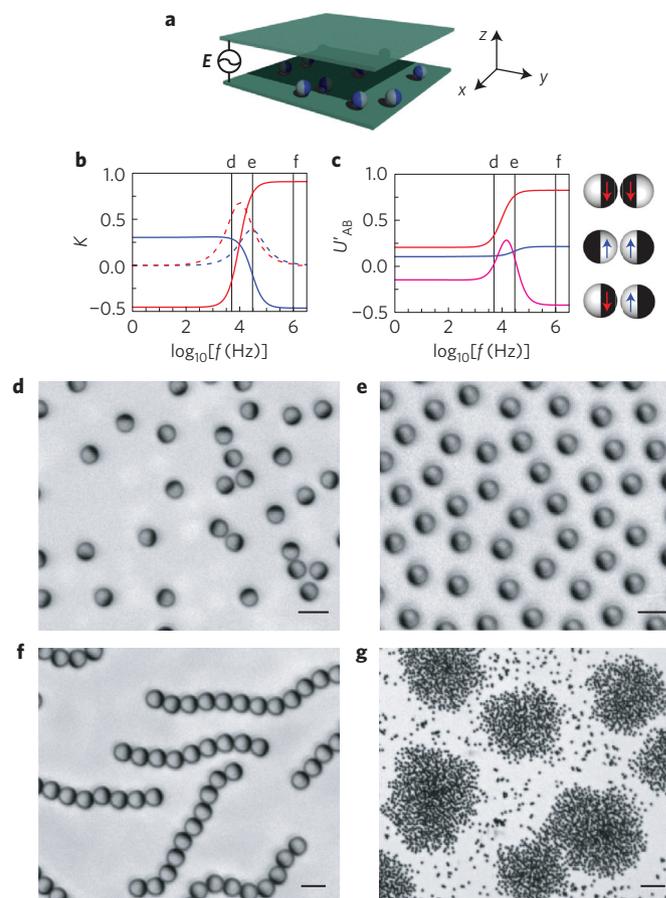
(Fig. 2c). Particles align during binary collisions (statistics shown in Supplementary Fig. 2) and further organize into coherent swarms (Fig. 2e). Finally, once the frequency reaches the megahertz range (Fig. 2f), ions barely follow the rapidly oscillating field, and the inherent material response dominates. The strong, opposite dipoles of the metallic and dielectric hemispheres yield head-to-tail attraction, producing the active chains predicted in Fig. 1a. Collisions between active chains lead to temporary alignment, but chain flexibility precludes their collective polar swarms that have been seen in other systems[9]. For each individual chain, any particle along it tends to align its orientation with those of adjacent particles in front and behind through the interactions between their shifted dipoles, so that chains remain straight unless perturbed by their environment. Collision of the leading particle with another chain or an obstacle reorients that particle and initiates a new straight segment along a different direction, creating a
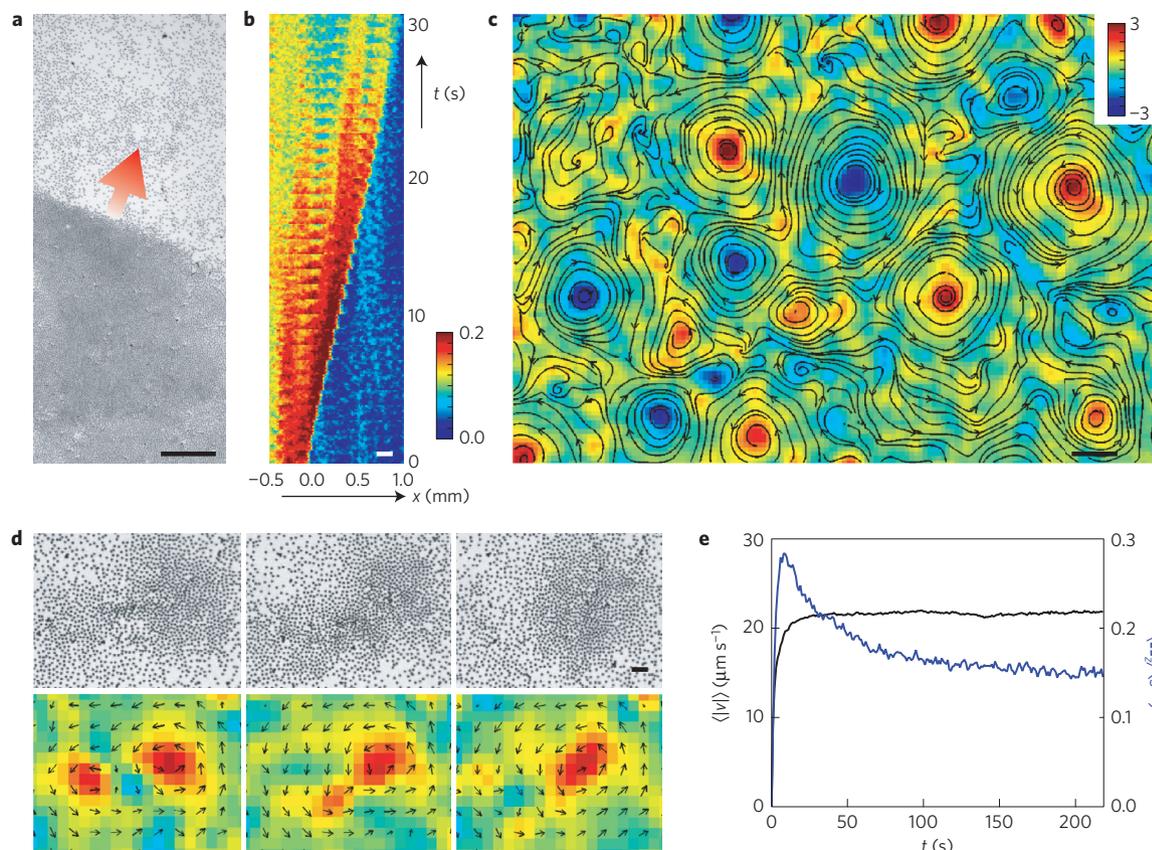
Figure 3 | Time evolution in the swarming state. a, Representative 2D snapshot of a polar wave at a given time, migrating in the direction indicated by the arrow. Initial particle area fraction $\phi_0 = 0.13$. **b**, Kymogram showing the propagation of the wave in panel **a**, with the vertical axis representing time (t) and the horizontal axis representing translation along the direction of migration x. Colour coding denotes averaged local area fraction $\phi(x)$, ranging from 0 to 0.2. The constant slope indicates a constant travelling velocity of the wavefront. **c**, Illustration of the final state with multiple vortices in a dilute sample ($\phi_0 = 0.04$). Shown is the vorticity map $\omega_z(r)$, normalized by $\langle|\omega_z(r)|\rangle$ and overlaid with streamlines. **d**, Vortices with the same polarity merge. Top panels: experimental images; bottom panels: corresponding $\omega_z(r)$ and velocity field. The time difference between successive images is 7.0 s. Colour coding is the same as in **c**. Scale bars are 200 μm in **a–c** and 40 μm in **d**. **e**, Time evolution of in-plane average particle speed $\langle|v|\rangle$ (unit: μm s^{-1}) and average magnitude of enstrophy $\langle\Omega_z\rangle$ (unit: s^{-2}), for the sample shown in **c**.

kink in the chain (Supplementary Movie 7). These effects give the impression that the whole chain follows a trail when moving, but eventually the kink rounds due to the weak rigidity of the chain. This finite rigidity is also responsible for the nearly circular shape of continuously rotating rings, the active analogue of closed loops predicted for equilibrium dipolar polymerization[23]. Lastly, the cluster state (Fig. 2g and Supplementary Movie 8) is likewise observed when salt is added to tune the dipolar interaction to the appropriate range (Supplementary Fig. 3).

Beyond these predicted local arrangements, swarm states exhibit an intriguing hierarchical time dependence as they evolve to larger-scale structures. Initially, small coherent groups of particles nucleate in different locations and move in random directions. These collide and merge into huge waves (Fig. 3a and Supplementary Movie 9) sweeping over the field of view, a process involving tens of thousands of spheres heading in the same direction. Moreover, the wavefront propagates at a constant speed (Fig. 3b) up to 1.4 times faster than individual spheres in the wave, typical of a shockwave[2]. This shockwave arises as the polar wave continually recruits new particles from the random, dilute phase to the front of its directional migration. A simple phenomenological model captures the observed shockwave speed (Supplementary Fig. 4). These waves are transient: collisions between waves lead to vortices (Supplementary Fig. 5). In a dense system (initial area fraction $\phi_0 = 0.13$), giant vortices emerge as the final state (Supplementary Movie 10). But in systems with lower particle density ($\phi_0 = 0.04$), the

polar state is so transient that multiple vortices form immediately after the electric field is turned on, after which the system evolves to many isolated, stable vortices (Fig. 3c). Vortices with the same polarity merge over time (Fig. 3d) while neighbouring vortices with opposite polarities do not annihilate: by sharing a common flow in-between, they maintain stable configurations. Figure 3e quantifies the time evolution of a typical dilute system by the average particle speed $\langle|v|\rangle$ in the image plane and the average magnitude of enstrophy $\langle\Omega_z\rangle$ (ref. 24). $\langle|v|\rangle$ quickly rises to steady state as particle motions become coordinated and the number of collisions diminishes. $\langle\Omega_z\rangle$ first increases sharply, signifying the formation of numerous vortices, but gradually decreases as vortices merge. The stable final configuration presents neighbouring vortices all with opposite polarities.

The exact origin of vortex formation is yet unclear. Previous simulations demonstrated that two-particle alignment can generate a vortex state if combined with long-range attraction[25]. A possible source for this would be electrophoretic flow: in this high-frequency range, where Janus particles swim with their metallic sides forward, opposite to regular ICEP[15] observed at low frequency, the particles may pump flow from the x–y plane to the z axis and create a long-range hydrodynamic attraction.

Time evolution of the clustering process is also interesting to consider. Supplementary Fig. 6a shows a typical time sequence. Qualitatively it is reminiscent of classical phase separation processes[19] (Supplementary Fig. 6b): clusters grow either by
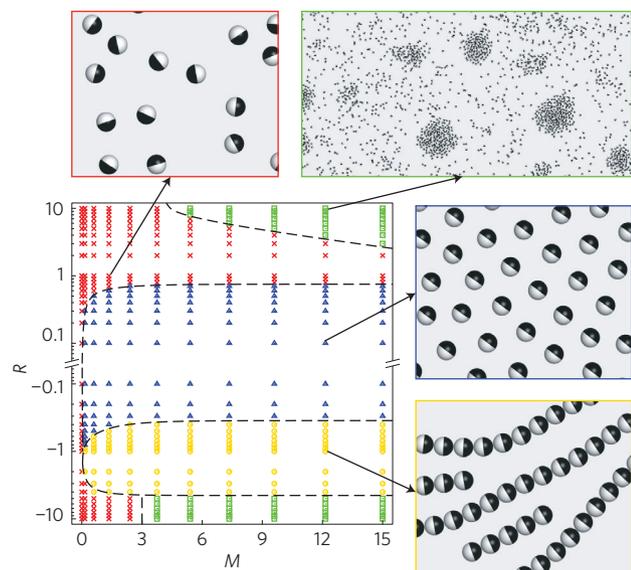
Figure 4 | Dynamic state diagram from 2D simulations. R is the ratio of the dipole moment on the trailing Janus hemisphere and the dipole moment on the leading hemisphere. M is the dipolar repulsive force between two spheres at contact, normalized by the swimming force. Simulation snapshots for the four different phases are shown, and the corresponding parameter choices (R, M) are indicated by the arrows. Only the cluster state is sensitive to M, because the nucleation of small clusters requires local reorientation of multiple particles, a process possible only if particles are given enough time to reorient before they separate again. The timescale of reorientation is determined by the competition between interaction strength and particle motility, precisely what is quantified by M.

merging or by an evaporation–condensation mechanism in which swimming particles leave small clusters and join larger clusters, similar to the Oswald ripening process of crystals. The hierarchical evolution in these active states underscores the rich dynamics in such active materials, which share some similarity with classical thermodynamic systems, but differ in other important ways.

To unify these observations, we systematically scan the parameter space via MD simulations (see Methods) that capture the experiment's quasi-2D feature and dipolar interactions controlled chiefly by just two factors, the strength and imbalance of dipolar interactions. We quantify the former by the ratio M of the dipolar repulsive force between two particles at contact to the swimming force, and the latter by the ratio R of the tail dipole to the head dipole. For simplicity and generality, the dipoles here are chosen to be real-valued rather than complex. Exploring the space spanned by R and M, with special attention to the phase boundaries, we generate the dynamic state diagram in Fig. 4. The swarm and chain states are insensitive to the particle motility for a wide range of M. Indeed, we estimate the state space for stable chain configurations via simple force calculations (Supplementary Fig. 7), which predict a stable R range (-6.7, -0.15), close to the measured R range (-5.0, -0.35). Likewise, the swarm state is stable as long as the magnitude of the head dipole is 1.25 times larger than that of the tail dipole. In contrast, the cluster state depends sensitively on particle motility, as faster particle motion leaves insufficient time for particles to reorient and organize into a cluster. We find fairly close correspondence between the experimental observations and the predictions from the simulated state diagram (Supplementary Discussion 9). Although the swimming speed and interparticle interactions are simultaneously changed by a single experimental parameter (such as field strength or frequency), combinatorial tuning of conditions and materials still makes it possible to explore the state diagram, as we have shown for the cluster phase using

altered ionic strength. The state diagram provides a general road map for experimental design in this particular system, but also is potentially generalizable to other systems.

The strategy presented here to organize collective active matter shows the potential of classic colloid science[26] to enrich the newer field of active matter. Expanding the metaphor that active matter can emulate living systems, we have demonstrated that a broad variety of collective, active states can be generated from a single species of Janus particle. The strategy, if one extrapolates beyond the electrostatic interactions (more specifically, dipolar interactions in the experiments) considered here, should hold for other forms of colloidal interactions that can be combined with the broken symmetry in the particle, such as steric forces owing to surface-coated polymers[26] and even hard-core interactions if the particle shape is asymmetric[27], and this study can be considered a first step in that direction. These states do not rely on the commonly employed but complex hydrodynamic interactions to produce collective motion, but instead stem predictably from pairwise interactions that are controllable and well studied in colloid science[4]. The design principle might be extended to program other motile elements. Many such can be imagined, from nanoparticles to energized granular particles[28], with the common element of avoiding the need for sophisticated algorithms to control collective assembly[10]. The experiments, presented here for convenient quasi-2D systems, illustrate more general principles, which we have validated by simulations not only in 2D but also in 3D.

Methods

Methods and any associated references are available in the online version of the paper.

References

1. Marchetti, M. C. *et al*. Hydrodynamics of soft active matter. *Rev. Mod. Phys.* **85**, 1143–1189 (2013).
2. Bricard, A., Caussin, J.-B., Desreumaux, N., Dauchot, O. & Bartolo, D. Emergence of macroscopic directed motion in populations of motile colloids. *Nature* **503**, 95–98 (2013).
3. Sanchez, T., Chen, D. T. N., DeCamp, S. J., Heymann, M. & Dogic, Z. Spontaneous motion in hierarchically assembled active matter. *Nature* **491**, 431–434 (2012).
4. Lu, P. J. & Weitz, D. A. Colloidal particles: crystals, glasses, and gels. *Annu. Rev. Condens. Matter Phys.* **4**, 217–233 (2013).
5. Wang, Y. *et al*. Colloids with valence and specific directional bonding. *Nature* **491**, 51–55 (2012).
6. Poon, W. C. K. From *Clarkia* to *Escherichia* and Janus: the physics of natural and synthetic active colloids. *Proc. Intl Sch. Phys. Enrico Fermi* **184**, 317–386 (2013).
7. Palacci, J., Sacanna, S., Steinberg, A. P., Pine, D. J. & Chaikin, P. M. Living crystals of light-activated colloidal surfers. *Science* **339**, 936–940 (2013).
8. Wang, W., Duan, W., Ahmed, S., Sen, A. & Mallouk, T. E. From one to many: dynamic assembly and collective behavior of self-propelled colloidal motors. *Acc. Chem. Res.* **48**, 1938–1946 (2015).
9. Schaller, V., Weber, C., Semmrich, C., Frey, E. & Bausch, A. R. Polar patterns of driven filaments. *Nature* **467**, 73–77 (2010).
10. Rubenstein, M., Cornejo, A. & Nagpal, R. Programmable self-assembly in a thousand-robot swarm. *Science* **345**, 795–799 (2014).
11. Snezhko, A. & Aranson, I. S. Magnetic manipulation of self-assembled colloidal asters. *Nature Mater.* **10**, 698–703 (2011).
12. Walther, A. & Müller, A. H. E. Janus particles: synthesis, self-assembly, physical properties, and applications. *Chem. Rev.* **113**, 5194–5261 (2013).
13. Zhang, J., Luijten, E. & Granick, S. Toward design rules of directional Janus colloidal assembly. *Annu. Rev. Phys. Chem.* **66**, 581–600 (2015).
14. Shah, A. A., Schultz, B., Zhang, W., Glotzer, S. C. & Solomon, M. J. Actuation of shape-memory colloidal fibres of Janus ellipsoids. *Nature Mater.* **14**, 117–124 (2015).
15. Gangwal, S., Cayre, O. J., Bazant, M. Z. & Velev, O. D. Induced-charge electrophoresis of metallodielectric particles. *Phys. Rev. Lett.* **100**, 058302 (2008).

16. Nishiguchi, D. & Sano, M. Mesoscopic turbulence and local order in Janus particles self-propelling under an ac electric field. *Phys. Rev. E* **92,** 052309 (2015).
17. de Gennes, P. G. & Pincus, P. A. Pair correlations in a ferromagnetic colloid. *Phys. kondens. Mater.* **11,** 189–198 (1970).
18. Vicsek, T., Czirók, A., Ben-Jacob, E., Cohen, I. & Shochet, O. Novel type of phase transition in a system of self-driven particles. *Phys. Rev. Lett.* **75,** 1226–1229 (1995).
19. Wittkowski, R. *et al*. Scalar ϕ^4 field theory for active-particle phase separation. *Nature Commun.* **5,** 4351 (2014).
20. Buttinoni, I. *et al*. Dynamical clustering and phase separation in suspensions of self-propelled colloidal particles. *Phys. Rev. Lett.* **110,** 238301 (2013).
21. Yethiraj, A. & van Blaaderen, A. A colloidal model system with an interaction tunable from hard sphere to soft and dipolar. *Nature* **421,** 513–517 (2003).
22. Zhang, J., Yan, J. & Granick, S. Directed self-assembly pathways of active colloidal clusters. *Angew. Chem. Int. Ed.* **55,** 5166–5169 (2016).
23. Rovigatti, L., Russo, J. & Sciortino, F. No evidence of gas-liquid coexistence in dipolar hard spheres. *Phys. Rev. Lett.* **107,** 237801 (2011).
24. Wensink, H. H. *et al*. Meso-scale turbulence in living fluids. *Proc. Natl Acad. Sci. USA* **109,** 14308–14313 (2012).
25. D'Orsogna, M. R., Chuang, Y. L., Bertozzi, A. L. & Chayes, L. S. Self-propelled particles with soft-core interactions: patterns, stability, and collapse. *Phys. Rev. Lett.* **96,** 104302 (2006).
26. Israelachvili, J. N. *Intermolecular and Surface Forces* 3rd edn (Academic, 2011).
27. Glotzer, S. C. & Solomon, M. J. Anisotropy of building blocks and their assembly into complex structures. *Nature Mater.* **6,** 557–562 (2007).
28. Kumar, N., Soni, H., Ramaswamy, S. & Sood, A. K. Flocking at a distance in active granular matter. *Nature Commun.* **5,** 4688 (2014).

Author contributions

J.Y. and S.G. initiated this study. J.Y., J.Z. and C.X. performed the experiment and analysed the data. M.H. and E.L. designed the model and performed the simulation. All authors contributed to the writing of the paper.

Additional information

Supplementary information is available in the online version of the paper. Reprints and permissions information is available online at www.nature.com/reprints. Correspondence and requests for materials should be addressed to E.L. or S.G.

Competing financial interests

The authors declare no competing financial interests.

Methods

Simulation procedure. We perform overdamped molecular dynamics simulations using the LAMMPS package to investigate active motions of Janus colloids (radius a). For the quasi-2D simulations, particles with an area fraction of 0.05 are confined to the plane and move within a square, periodic domain of side length $200a$. Each particle carries two dipoles shifted away from the particle centre by $d = (3/8)a$ towards its leading and trailing hemisphere, respectively. Both are oriented perpendicular to the x–y plane. For the 3D simulations, particles with a volume fraction of 0.0077 (except for the swarm state, volume fraction = 0.0157) move within a cubic, periodic domain of side length $50a$. To show generality, each particle in the 3D case carries two charges off-centre by $d = a/2$ instead, interacting via screened Coulomb interactions with Debye length $\lambda_D = a/6$.

We employ reduced units, with the particle diameter $D = 3\,\mu m$ as length unit, the particle mass $m = 3.74 \times 10^{-14}$ kg as mass unit and the thermal fluctuations $k_B T = 4.11 \times 10^{-21}$ J as energy unit. This yields a time unit of 0.009 s. Given the dynamic viscosity η of water, the spherical particles experience a frictional force $F_t = -\zeta_t \mathbf{v}$ and a torque $T_r = -\zeta_r \boldsymbol{\omega}$, with translational drag coefficient $\zeta_t = 6\pi\eta a = 6.06 \times 10^3$ and rotational drag coefficient $\zeta_r = 8\pi\eta a^3 = 2.02 \times 10^3$ in reduced units. According to the reciprocal theorem[29], the self-propulsion of the particle can be translated into motion driven by an external force $F_{ex} = \zeta_t \mathbf{v} = 3.64 \times 10^2$ (corresponding to a steady-state velocity $v \approx 20\,\mu m\,s^{-1}$). In addition to electrostatic interactions, particles also interact through their excluded volumes, modelled via a shifted–truncated Lennard-Jones interaction with $\sigma = 1$, $\varepsilon_{LJ} = 1$ and cutoff $r_c = 2^{1/6}$. All simulations proceed for at least 10^8 steps, with time step 5×10^{-4} ($= 4.5 \times 10^{-6}$ s).

Particle synthesis. Janus particles are created using directional deposition of metal onto dry colloidal particles in vacuum[30]. Typically, a 2% suspension (20 μl) of 3-μm-diameter silica particles (Tokuyama) is spread on a half glass slide (1.0×1.5 inch^2), pretreated with Piranha solution, and dried to form a submonolayer. Next, a thin titanium coating (35 nm) followed by a SiO$_2$ film (15 to 20 nm) is deposited vertically using electron-beam deposition, at 3×10^{-6} torr and a deposition rate of 0.5 Å s^{-1}. The monolayer is washed thoroughly with deionized (DI) water and isopropyl alcohol, and then sonicated in 15 ml DI water for 90 s to collect the particles. Further sonication for 1 h is applied to break up any aggregates, ensuring the production of discrete Janus spheres. After sedimentation for another hour, the concentrated suspension at the bottom of the centrifuge tube is used for the next step.

Protocol of electric-field-induced active self-assembly. To apply an electric field, we sandwich the particles between two coverslips coated with indium tin oxide (ITO, from SPI). The ITO-coated coverslips are further coated with 25 nm SiO$_2$ using electron-beam deposition to prevent surface absorption of the particles. A thin strip on one side of the ITO-coated coverslip is left uncoated during the SiO$_2$ deposition, which is later connected to copper tapes and further to a function generator (Agilent 33522A). The two ITO-coated coverslips are separated by a spacer (Grace, Biolab, SecureSeal) about 120 μm in thickness, with a 9-mm-diameter hole. Imaging is done on a Zeiss inverted microscope using transmission mode. A ×5 objective is used for large-scale imaging and a ×40 long-working-distance objective is used for the zoomed-in view. Movies are recorded using a complementary metal-oxide-semiconductor (CMOS) camera (Edmund Optics 5012M GigE). A square wave of 10 V is used for most experiments.

Image analysis. Custom-written Matlab codes were developed to analyse the experimental movies. For the zoomed-in views, we tracked the position and orientation of each individual Janus sphere[30]. To track the large-scale pattern evolution, we developed customized codes for particle image velocimetry (PIV). To avoid pixel-locking effects, a hybrid method is used to find the displacement of a subwindow: first, using 2D Fourier-transform-based correlation, the integers of the displacement vector are obtained. Next, a local search with a step size of 0.1 pixel is performed to improve the accuracy. Pixel-locking effects are minimized in this way. The typical interrogation window size is 32 × 32 pixels^2 (40.5 μm^2), with a 50% overlap. Arrows on the figures represent averaged values from 2 × 2 subwindows. The local area fraction is calculated by counting the number of particles which appear as black dots in images with a ×5 objective. To generate the spatio-temporal plot and analyse the local area fraction profile of the polar wave, the images are rotated to place the direction of the wave along the x axis. $\phi(x)$ is then the area fraction averaged along the direction perpendicular to the wave motion.

Code availability. Custom Matlab codes for PIV and binary collision tracking are available on www.nature.com, including detailed instructions.

References

29. Happel, J. & Brenner, H. *Low Reynolds Number Hydrodynamics: With Special Applications to Particulate Media* Ch. 3 (Prentice-Hall, 1965).
30. Yan, J., Bloom, M., Bae, S. C., Luijten, E. & Granick, S. Linking synchronization to self-assembly using magnetic Janus colloids. *Nature* **491,** 578–581 (2012).